Journal of Non-Crystalline Solids 440 (2016) 1–6

Contents lists available at ScienceDirect

Journal of Non-Crystalline Solids

journal homepage: www.elsevier.com/locate/jnoncrysol

Premelting and cation mobility in simple silicates: Contrasting the dynamics in the crystalline and molten state

B. Mantisi, M. Micoulaut *

Laboratoire de Physique Théorique de la Matière Condensée, Paris Sorbonne Universités UPMC, Boite 121, 4, place Jussieu, 75252 Paris Cedex 05, France

ARTICLE INFO

Article history:
Received 19 January 2016
Received in revised form 24 February 2016
Accepted 26 February 2016
Available online 11 March 2016

Keywords:
Sodium silicate crystals
Molecular dynamics
Glassy
Relaxation
Premelting

ABSTRACT

The dynamics of atomic species in crystalline and molten sodium disilicate $2SiO_2$–Na_2O is investigated and analyzed from molecular dynamics simulations. A clear signature of premelting is detected at $T = T_0 \approx 800$ K that leads to a complete melting of the Na subnetwork while preserving the (Si,O) one. For higher temperatures, it is found that while the global behavior in terms of transport is rather similar between both states with values for the diffusivity and diffusion activation energies that are close, the nature of the ion motion is radically different. At low temperature, the motion of Na atoms in premelted crystals is, indeed, almost two-dimensional between layers of $SiO_{4/2}$ connected tetrahedra but with increasing temperature, the dynamics becomes essentially 3D. The analysis of the intermediate scattering function within the framework of trap models confirms the analysis.

1. Introduction

The diffusion and dynamics of species is of great interest in both crystalline and amorphous materials. Recently, it has been found that atomic motion and diffusion can be measured in glasses even at room temperature [1,2], and corresponding relaxation times appear to be strongly decoupled from viscosity, while also being substantially influenced by the network structure. From molecular simulations, such temperatures below the glass transition temperature are out of reach, and the related relaxation time of diffusive régime is beyond the computer timescale.

In crystals, the same situation holds and is probably enhanced as compared to supercooled liquids and glasses, at least experimentally. Both Raman and electrical conductivity measurements [3,4] at temperatures slightly below the melting point indicate, indeed, that premelting effects of typical silicates in the solid state ($CaSiO_3$, Na_2SiO_3) are associated with an enhanced dynamics of cations, and this high mobility sets in several hundreds of degrees below the melting point. In sodium silicates, such effects seem to be associated with an extensive deformation of the silicate chains [4], as evidenced from the similarity of the Raman spectra of the crystalline and liquid phases.

There are more basic aspects regarding these questions which belong to the topic of lattice diffusion, also termed bulk or volume diffusion. Atomic diffusion within a crystalline lattice occurs, indeed, by various mechanisms among which diffusion occurring through interstitial motion or by substitution, the former being found when the diffusing ion moves in between the lattice structure of another crystalline element [5]. Conversely, in substitutional lattice diffusion, atoms can only move by substituting place with another atom, a situation that is favored when point vacancies throughout the crystal lattice are available. As a result, such mechanism depends substantially on the degree of order that is found in the network structure whereas in glasses or supercooled liquids, the mobile ions can encounter a larger number of sites between jumps, leading to different relaxation scenarios [6]. One may therefore wonder to what extent the presence of a crystalline sub-lattice can affect the ion dynamics at low temperature. This is the purpose of the present contribution.

Using molecular simulations we study and analyze the difference in behavior of the diffusivity and the glassy relaxation between a regular supercooled liquid obtained from a progressive melt quench from high temperature, and a crystalline structure which contains a strong molecular ordering. Results on a model $2SiO_2$–Na_2O sodium disilicate show that while the diffusivity is nearly the same at temperatures close to the melting point, the Na diffusivity is strongly influenced at low temperature by the sheet-like structure of the starting di-silicate crystalline polymorph, and leads in fact to features of premelting, i.e. sodium motion is enhanced at temperatures below the melting point which is then characterized by a complete breakdown of the crystalline (Si,O) network. In addition, it is found that the sodium motion evolves from a 2D intra-layer diffusive régime towards a 3D inter-layer régime. An analysis of the corresponding glassy relaxation from trap models confirms this behavior independently, while also suggesting that such features are strongly influenced by the related silica network structure.

---

* Corresponding author.
E-mail address: mmi@lptl.jussieu.fr (M. Micoulaut).

http://dx.doi.org/10.1016/j.jnoncrysol.2016.02.025

2. Simulation methods

Using MD simulations, we have studied at P = 0 in a (N,P,T) Ensemble a 3020-atom system having as starting structure crystalline δ-$Na_2Si_2O_5$. This structure [7] is one of the four possible polymorphs of sodium di-silicate $2SiO_2$–Na_2O that forms at ambient pressure [8]. Its structure (space group P_{12_1}/n_1) has been determined from X-ray diffraction and has a sheet-like structure (Fig. 1) with a short lattice constant of about 4.9 Å. The Na atoms are found between layers of a silica-rich network which is a common feature of several other metastable crystalline polymorphs obtained [9,10].

The atoms interact via a two-body Teter potential [11,12] which describes very accurately the structure [12,13,14] and the dynamics [13] of corresponding liquids and glasses. It has been found, indeed, that real and reciprocal space functions are very well reproduced such as the pair correlation function or the structure factor [12,14]. Similarly, the calculated diffusion constants and viscosity at zero pressure have been found to be very close to their experimental counterparts [13]. Concerning the diffusion constants, their values have been furthermore found to be at least one order of magnitude different when compared to alternative potentials [15].

The equations of motion have been integrated using a leap-frog Verlet algorithm with a time-step of 2 fs. Starting from 300 K, we have progressively heated the crystal up to 4000 K with a heating rate of 1 K/ps, and then subsequently quenched from the liquid down to room temperature at the same rate.

At the target temperatures of our study (see below), we have simulated trajectories up to 3 ns in the NVT Ensemble, and have discarded the first ns for the statistical analysis.

3. Results

3.1. Energy behavior

Fig. 2 represents the calculated energy E^* (T) of the crystalline and liquid systems. To obtain this reduced energy E^* (T), we have subtracted from the total calculated energy E(T) the contribution 9RT/2 arising from the vibrational motion. This subtraction only permits to blow up certain interesting trends (transitions) which are otherwise hidden by the linear increase of E(T) due to the atomic vibrations.

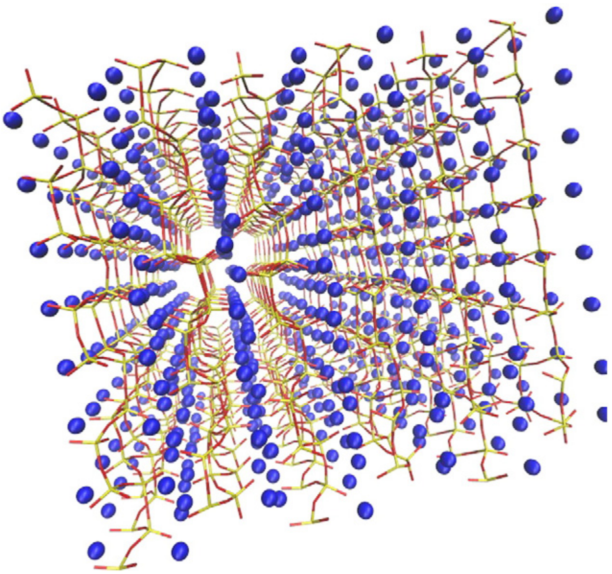

Fig. 1. An atomic snapshot of the initial crystalline structure of sodium di-silicate δ-$Na_2Si_2O_5$. Sodium atoms are in blue and occupy periodic positions between layers of the remaining (Si,O) network structure which is shown with red and yellow bars, respectively.

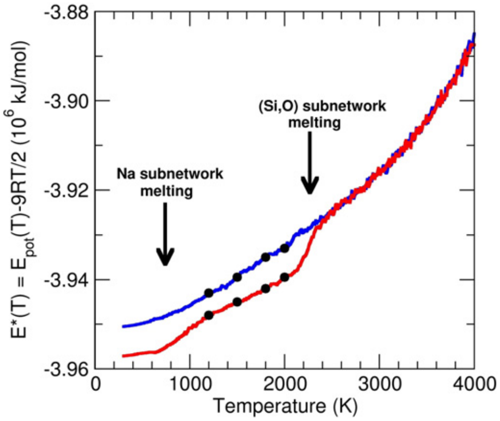

Fig. 2. Behavior of the reduced energy E^*(T) as a function of temperature in crystalline/liquid (δ-$Na_2Si_2O_5$, red) and liquid/supercooled NS2 (blue). The black dots signal the studied systems throughout this article at T = 1200 K, 1500 K, 1800 K and 2000 K.

Starting from the crystalline δ-$Na_2Si_2O_5$ polymorph at low temperature, a progressive heating (red curve) leads to a smooth increase of E^*(T) which exhibits two marked jumps at $T_0 \approx 800$ K and at $T_m \approx 2200$ K corresponding to the melting of the Na subnetwork (premelting) and the full (Si,O) network melting (experimentally 1148 K [8]), respectively. The former induces an important motion that is gained by the sole ionically interacting Na cations, the remaining (Si,O) network structure still being found in partial crystalline order. An evaluation of the mean-square displacement $<r_i^2(t)>$ supports this claim because an important growth in Na motion is detected across the transition at T_0, whereas the nearly unchanged behavior of $<r_{Si}^2(t)>$ and $<r_O^2(t)>$ signals that the (Si,O) part of the crystalline structure has not melted (Fig. 3a). In fact, both $<r_{Si}^2(t)>$ and $<r_O^2(t)>$ display a plateau behavior indicating that the motion is restricted to a mean square displacement of about less than 1 $Å^2$. Conversely, $<r_{Na}^2(t)>$ exhibits a linear behavior for t > 5 ps that is indicative of a diffusive regime.

The salient phenomenology of the glass transition is then recovered. In fact, upon cooling from 4000 K down to low temperature, the system becomes supercooled below T_m, and both curves (heating and cooling) now differ for $T < T_m$, consistently with the current experimental observation of supercooled melts. Finally, at some temperature $T_g \approx 1000$ K corresponding the intercept between the low temperature and high temperature linear expansion of E^*(T), an approximate glass transition temperature can be defined. The obtained structure is fully disordered, and corresponding partial pair correlation functions (not shown) are found to be, indeed, representative of a glassy structure.

In the forthcoming, we focus on four data points at T = 1200 K, 1500 K, 1800 K and 2000 K and compare the dynamics of the supercooled liquid (blue curve in Fig. 2) with its corresponding premelted crystal (red curve, termed crystal hereafter).

3.2. Ion dynamics

We first focus on the behavior of the dynamics of the species at these four temperatures in both systems, i.e. the supercooled liquid and the crystal.

First, we calculate the mean square displacement (msd) of the atoms:

$$r^2(t) = \frac{1}{N_\alpha}\sum_{i=1}^{N_\alpha}\left|\mathbf{r}_i t - \mathbf{r}_i(0)\right|^2 \qquad (1)$$

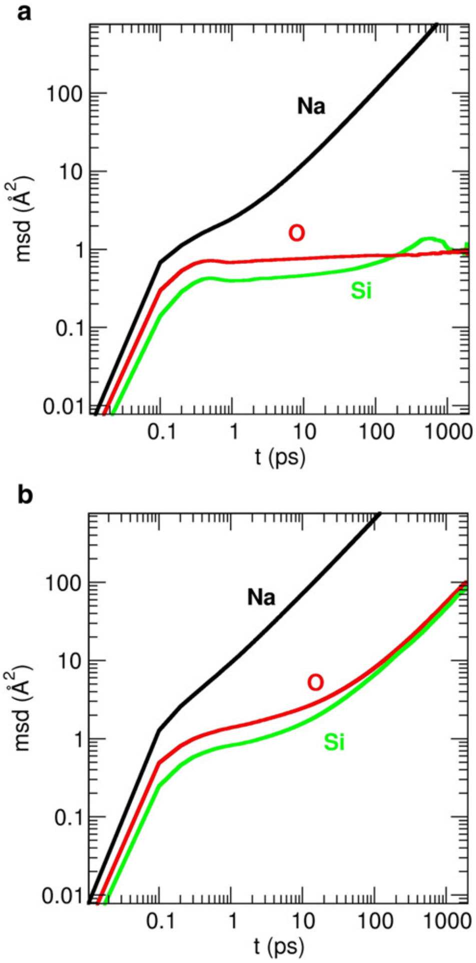

Fig. 3. Behavior of the mean-square displacement $<r_i^2(t)>$ ($i = Na,Si,O$) at 1200 K (a) and 1800 K (b), showing the onset of diffusion for Na-species only at low temperature.

A typical behavior is shown in Fig. 3 which indicates that when $T > T_0$, the sodium atoms exhibit a diffusive behavior at long times ($t > 20$ ps for 1200 K) similarly to what is found in the supercooled liquid [13]. This behavior contrasts with the msd calculated for the network species which display a plateau-behavior typical of solids, glasses or crystals, and its value ($r^2(t) \approx 0.4-0.5$ Å) roughly corresponds to typical values expected from the Lindemann criterion for crystals [16], i.e. $r^2(t) \approx 0.01\, a^2$ where a is the cell length of the crystal (here 4.9 Å [8]). As the temperature is increased, the msd of Si and O species can grow to eventually lead to a diffusive regime at temperatures close to the melting point (Fig. 3 bottom).

From the long-time limit of the msd (Fig. 3), we calculate the diffusivity D_{Na} of the sodium ions using the Einstein relationship $D = r^2(t)/6t$ at different temperatures. Results are found to agree with experimental measurements from Gupta and King [17] and from Negodaev [18] performed in the liquid state (Fig. 4), while being also consistent with the data of Johnson et al. [19]. In fact, the calculated D_{Na} at various temperatures is close to the one determined experimentally, this being true up to $10^4/T \approx 6$–8. One furthermore notices that the sodium diffusivity displays an Arrhenius behavior $D = D_0 \exp[-E_A/k_BT]$ that is, in addition, very close between the crystalline and the supercooled state with activation energies that are nearly identical, i.e. we find $E_A = 0.45(7)$ and $E_A = 0.49(3)$ for the crystal and the liquid, respectively.

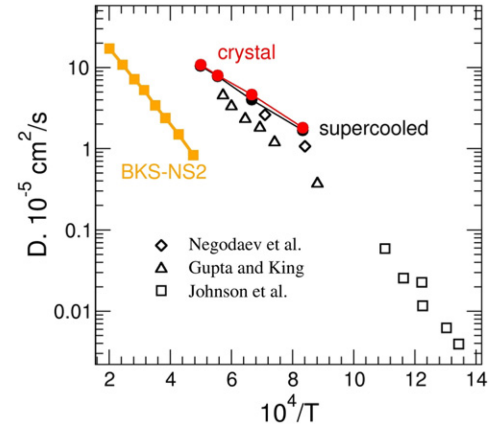

Fig. 4. Arrhenius plot of sodium diffusivity of crystalline and supercooled NS2, compared to experimental findings (open symbols, [17–19]) and to results from a simulation of supercooled NS2 using an alternative potential (BKS) [21].

3.3. Ion relaxation

To furthermore decode the nature of the ion dynamics, we compute the intermediate scattering function $F_s(k,t)$ defined by:

$$F_s(k,t) = \frac{1}{N}\sum_{j=1}^{N} \exp[ik.(r_j(t) - r_j(0)] \tag{2}$$

which follows the Fourier components of density correlations, and permits to characterize the slowing down of the relaxation as the temperature is decreased, while also providing the information about structural relaxation in the long-time limit. In Fig. 5, we represent $F_s(k,t)$ for the supercooled liquid at $k = k_{max} = 3.04$ Å^{-1}, the principal peak position [14,20] of the static structure factor $S(k)$. At high temperature (2000 K), both ion and network forming species (oxygen) relax to

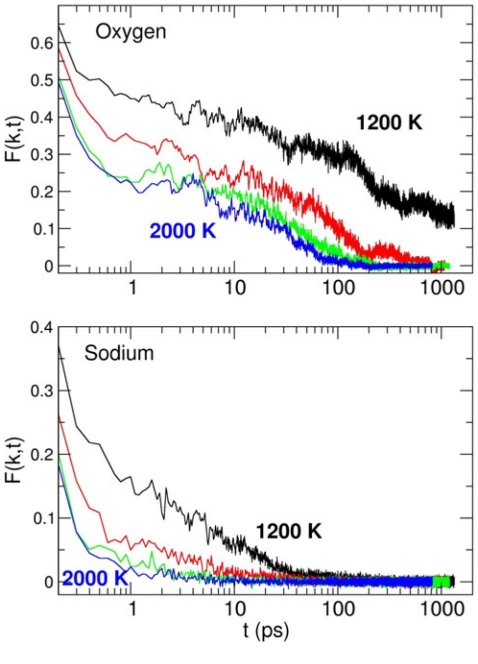

Fig. 5. Oxygen (top) and sodium (bottom) intermediate scattering function $F_s(k,t)$ of supercooled liquid NS2 at different temperatures (2000 K, 1800 K, 1500 K, 1200 K) and at a wavevector $k = k_{max}$ where k_{max} corresponds to the position of the principal peak of the static structure factor $S(k)$.

equilibrium on the computer timescale (2 ns), and one has $F_s(k,t) = 0$ at $t > 100$ ps and $t > 1$ ps for oxygen and sodium, respectively.

At lower temperatures, one observes a slowing down of the dynamics and the usual two-step relaxation behavior with a β-relaxation plateau that sets in for the network-forming species [21]. Conversely, the sodium related intermediate scattering function continues to decay to zero even at low temperature (1200 K), a feature that is consistent with the fact that the diffusive regime is still detected at this temperature.

When the relaxation dynamics is being compared between the crystalline and the supercooled state (Fig. 6), one acknowledges small differences that are detected in the way $F_s(k,t)$ decays to zero in the long time limit. Even at high temperature (2000 K), we note that the supercooled liquid relaxes differently, as detected in the time domain of around 1 ps. Such differences are emphasized at low temperatures and for both régimes, the β-relaxation plateau at 1–10 ps and the structural α-relaxation regime, now differ more markedly.

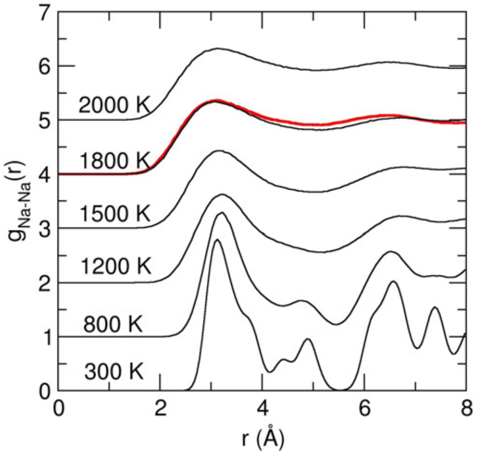

Fig. 7. Na–Na pair correlation function $g_{NaNa}(r)$ in premelted NS2 at different temperatures. The red curve shows the corresponding function in supercooled NS2 at 1800 K. The gap at $r \approx 5.8$ Å on the bottom curve signals the interlayer distance of δ-$Na_2Si_2O_5$.

4. Discussion

An inspection of the atomic snapshots and the full MD trajectory indicates that at low temperature, the nature of the ion motion is substantially different as compared to the one at higher temperature and in the supercooled state. In fact, once premelting has been achieved ($T > T_0$), the subnetwork made of sodium atoms becomes disordered and is typical of a liquid with weak differences when the corresponding structural correlations (i.e. the pair correlation function $g_{NaNa}(r)$) are being compared to the supercooled analogue (Fig. 7). Here, it is seen, indeed, that both functions exhibit the same peak at $r = 3.2$ Å corresponding to the first Na–Na correlating distance. However, there is a major difference that emerges from the inspection of the trajectories. In fact, without any softening of the silica network at low temperature, the motion of the sodium atoms in the crystal appears to be essentially two-dimensional as Na ions mostly explore the space defined between the layers of $SiO_{4/2}$ connected tetrahedra (Fig. 1).

In order to further analyze the dynamics, we calculate the mean-square displacement using Eq. (1) by setting the positions to: $\mathbf{r}_i(t) = \mathbf{r}_i^{\parallel}(t) + \mathbf{r}_i^{T}(t)$ with $\mathbf{r}_i^{T}(t)$ being the projected positions perpendicular to the layer direction of the crystalline lattice (Fig. 1), whereas $\mathbf{r}_i^{\parallel}(t)$ are those being parallel to the layer direction. This allows calculating a msd that is reduced to the inter-layer space in order to probe the 2D dynamics at low temperature. Fig. 8 shows corresponding results for two typical temperatures. First, we note that for all temperatures the 3D and 2D calculation differs as long as $r^2(t) < d_0$ with $d_0 \approx 5.80$ Å the interlayer distance, a situation that is met in the ballistic regime at short times when there is no spatial restriction due to the layered network structure, and when effects due to $\mathbf{r}_i^{T}(t)$ are active. For longer times and low temperature, there is no difference between a full account of all directions of ion motion (3D) and a calculation restricting the dynamics to the inter-layer space (2D, i.e. using $\mathbf{r}_i^{\parallel}(t)$ solely in Eq. (1)). This means that the dynamics is, in fact, restricted to a motion in 2D space as depicted from the accumulated snapshots (inset of Fig. 8), and only a very few Na atoms are able to move to the next interlayer space by substitutional lattice diffusion. The situation contrasts with the one obtained at higher temperatures (1800 K) where now the effect of interlayer motion (i.e. $\mathbf{r}_i^{T}(t)$) becomes significant, and the two calculated msds (2D and 3D) now differ. Taken together, these results indicate that with increasing temperature, a threshold takes place between a 2D intralayer motion and a 3D motion that is favored by the progressive softening of the silica chain network structure due to thermal activation. These conclusions certainly depend on the used MD timescale but even at the nanosecond one, the fraction of Na atoms being able to evolve in 3D is negligible as compared to those displaying the intra-layer motion.

The glassy relaxation that manifests from the decay of the intermediate scattering function can be analyzed and particularly the long-time behavior for which $F_s(k,t)$ is usually fitted with a stretched

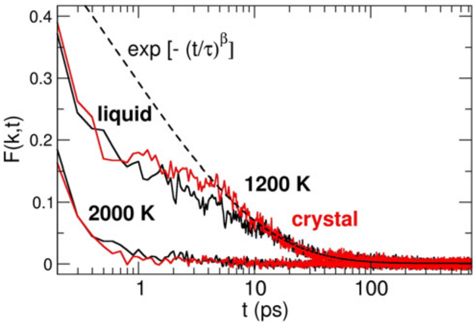

Fig. 6. Sodium intermediate scattering function $F_s(k,t)$ of supercooled liquid (black) and crystalline (red) NS2 at two different temperatures (2000 K, 1200 K) and at a wavevector $k = k_{max}$ where k_{max} corresponds to the position of the principal peak of the static structure factor S(k). The broken line shows a fit using a stretched exponential that permits having β and τ as a function of temperature in both states.

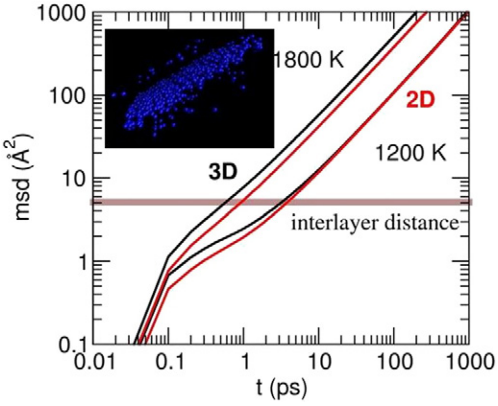

Fig. 8. Sodium msd at 1200 K and 1800 K in premelted NS2. The msd has been calculated in 3D (black curves, same as Fig. 3) and in 2D (red curves, see text for details). The interlayer distance of δ-$Na_2Si_2O_5$ (≈5.80 Å, see also Fig. 7) is signaled. The inset shows the accumulated snapshots for a single Na layer at 1200 K after 2 ns, indicating that most of the Na motion is restricted to the interlayer space.

exponential function of the form exp.[$-(t/\tau)\beta$] where τ is the structural α-relaxation time and β is the Kohlrausch exponent (broken line in Fig. 6). Results of the fit which lead to the evolution of τ and β with temperature, are displayed for both the crystalline and supercooled state (Fig. 9). It is found that τ increases as T decreases, consistently with the slowing down of the relaxation signaling the onset of glassy behavior, this trend being found for both states. For the premelted systems and although the (Si,O) continues to display structural ordering, this result is not surprising because the Na subnetwork has all the features of a supercooled liquid with a disordered structure (Fig. 7), including glassy behavior. The trend of β with temperature also appears to display some interesting features, especially for the crystalline state, as discussed below. However, we note that the corresponding activation energies for relaxation time are now substantially different, a situation that contrasts with the findings for diffusivity (Fig. 4). In fact, the activation energy for the Na relaxation time in the crystalline state is found to be $E_A = 1.09$ eV, i.e. higher than the one found for diffusivity ($E_A = 0.45$ eV). The situation differs from the one encountered for the supercooled liquid for which E_A is very similar, i.e. 0.54 eV and 0.49 eV for relaxation time and diffusivity respectively. This difference signals that the corresponding Stokes–Einstein (SE) relationship, i.e. $D \propto T/\tau$, must be broken in the crystalline premelted state. A representation of D as a function of T/τ (inset of Fig. 9a) shows indeed that while SE can be considered as valid at high temperatures in the supercooled liquid, this relationship does not hold at lower temperatures (1200 K, 1500 K) as usually found for deeply supercooled liquids [22,23], and on average one finds for a fractional SE exponent fulfilling $D \propto (\tau/T)^{\gamma}$ a value of $\gamma = -0.65$, i.e. quite similar to other glass-forming systems having $\gamma \approx -3/5$ [24]. On the other hand, for the premelted crystal, we do not find any sort of SE behavior, this being true even at high temperature, and a corresponding fractional SE exponent is found to be equal to $\gamma = -0.38$. The ordering due to the (Si,O) network structure is believed to play a key role in the breakdown of the SE relationship at all temperatures. In fact, since the solid-like character of the crystal enhances the decoupling of diffusivity and viscosity (or relaxation time), on the overall, it is not surprising that the small motion of the (Si,O) atoms lead to a decrease of the fractional exponent in the crystal.

Finally, such dramatic changes can be analyzed from the behavior of the Kohlrausch exponent β (Fig. 9b) which reflects the degree of cooperativity of the Na ions in the system, a smaller value for β being indicative of a larger collective behavior of cation motion. From Fig. 9, one can therefore argue that collective behavior is enhanced in the crystal as the temperature decreases because of the important decrease of β, from a value of 0.50 at 1200 K to a value of 0.37 at 2000 K. On the other hand, for the liquid NS2, a mild growth is obtained upon temperature increase, a result that is consistent with the fact the Kohlrausch exponent should approach 1 at high temperatures, and reduces as T decreases to T_g, the reduction being usually associated with the contraction of configuration space [25] in the supercooled liquid and its eventual stabilization due to structural arrest near $T = T_g$.

An interesting connection with network dimensionality is also provided [26], and models of traps [27,28] for tracer diffusion in a D-dimensional lattice show that β is related to the network dimensionality D via $\beta = D/(D + 2)$, a result that is satisfied for various molecular supercooled liquids and glasses [28]. In the present simulated premelted crystal, one finds indeed a rather high value for β at low temperature when the atomic motion of the sodium atoms is restricted to the space defined by two silica layers. For higher temperatures, β is found to be much closer to the predicted value of $\beta = 3/7 = 0.42$ [26] which is typical of a relaxation dominated by 3D long-range pathways, a result that has received some recent support both from experiments [29] and from simulations [30]. The situation found for the premelted NS2 system seems in line with the fact that once the relaxation of the Na atoms occur over several layers and become 3D, such long-range pathways must become important.

5. Conclusion

In the present contribution, we have investigated the dynamics of two different states of NS2, a supercooled liquid for which the structure is fully disordered and a premelted system having a disordered Na subnetwork embedded in a crystalline silica network that melts completely at a numerical melting temperature of 2200 K. Such investigations have some interest in the field of Earth sciences because certain crystalline compounds such as pseudowollastonite ($CaSiO_3$) or sodium metasilicates display premelting, i.e. a substantial increase of ionic diffusivity and conductivity several hundreds of degrees below the melting temperature, with obvious implications in geosciences. The present findings indicate that, indeed, premelting occurs at around 800 K that results in the melting of the Na sub-network as detected from the evolution of the energy with temperature. Investigations of this kind have

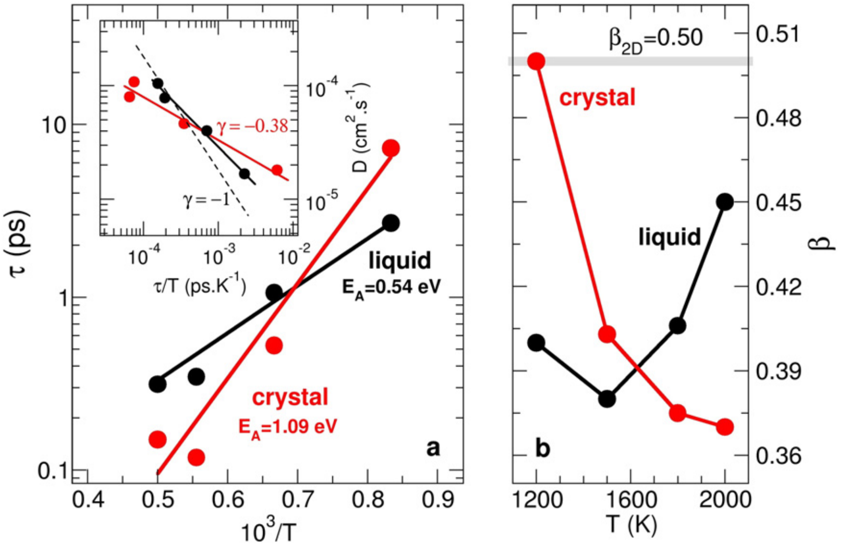

Fig. 9. Behavior of the relaxation time τ (a) and Kohlrausch exponent β (b) extracted from a stretched exponential fit of the intermediate scattering function $F_s(k,t)$. The inset shows a log–log plot of sodium diffusivity as a function of τ/T in order to check for the validity of the Stokes–Einstein (SE) relation. The broken line fulfills $D \propto (\tau/T)^{-1}$ ($\gamma = -1$). Fractional SE exponent for the crystal is indicated ($\gamma = -0.38$).

also of major industrial importance. Indeed, little attention is typically given to the fundamentals of batch-to-melt conversion and the science of glass melting [31]. Here we have shown that a direct MD simulation can mimic the full glass preparation process, from the usual raw material (a crystalline polymorph) to the melt, and, ultimately to the glass by an appropriate quench. While the temperatures somewhat differ from those determined experimentally, it is important to emphasize that the overall phenomenology is reproduced, and that, interestingly, non-obvious effects do appear once the starting crystal is heated to temperatures larger than 800 K.

The dynamics of both states, crystalline and molted, has been analyzed and we have found that within the numerical timescales, the Na motion displays a change in dimension from 2D to 3D as the temperature is increased but with an activation energy that is found to be similar to the corresponding supercooled liquid. Confirmation of this dimensional change is found independently from an analysis of the Kohlrausch exponent β that is analyzed within the framework of trap models. The relaxation of the system is also found to be slightly different and a breakdown of the Stokes–Einstein relationship is found for the premelted state only, at all temperatures.

It would be interesting to check to what extent such results and conclusions have a general character and do not depend on the initial crystalline structure of the polymorph or its layered character. Other crystalline polymorphs of NS2 or even polymorphs of other sodium silicates could be investigated along the same lines, and work in this direction is in progress.

References

[1] B. Ruta, G. Baldi, Y. Chushkin, B. Rufflé, L. Cristofolini, A. Fontana, M. Zanatta, F. Nazzani, Nat. Commun. 5 (2014) 3939.
[2] M. Ross, M. Stana, M. Leitner, B. Sepiol, New J. Phys. 16 (2014) 093042.
[3] M.A. Bouhifd, G. Gruener, B.O. Mysen, P. Richet, Phys. Chem. Miner. 29 (2002) 655.
[4] P. Richet, B.O. Mysen, D. Andrault, Phys. Chem. Miner. 23 (1996) 157.
[5] Atomic diffusion in disordered materials, in: S.M. Balkanski, R.J. Elliott (Eds.),Theory and Applications, World Scientific, 1998.
[6] K. Funke, R.D. Banhatti, S. Brückner, C. Cramer, D. Wilmer, Solid St, Ionics 105 (195) (1998).
[7] V. Kahlenberg, G. Dörsam, M. Wendschuh-Josties, R.X. Fischer, J. Solid State Chem. 146 (1999) 380.
[8] V. Kahlenberg, Chimia 64 (2010) 716.
[9] A.K. Pant, Acta Crystallogr. B24 (1968) 1077.
[10] V. Kahlenberg, S. Rakic, C. Weidenthaler, Z. Krist. 218 (2003) 421.
[11] J. Teter, unpublished results.
[12] A.N. Cormack, J. Du, T.R. Zeitler, J. Non-Cryst. Solids 323 (2003) 147.
[13] M. Bauchy, B. Guillot, M. Micoulaut, N. Sator, Chem. Geol. 346 (2013) 47.
[14] M. Bauchy, J. Chem. Phys. 137 (2012) 044510.
[15] B.W.H. van Beest, G.J. Kramer, R.A. van Santen, Phys. Rev. Lett. 64 (1990) 1955.
[16] W.A. Phillips, U. Buchenau, N. Nücker, A.J. Dianoux, W. Petry, Phys. Rev. Lett. 63 (1989) 2381.
[17] Y.P. Gupta, T.B. King, Trans. Metall. Soc. Amer. Inst. Mech. Eng. 239 (1967) 1701.
[18] G.D. Negodaev, I.A. Ivanov, K.K. Evstop'ev, Elektrochemie 8 (1972) 234.
[19] J.R. Johnson, R.H. Bristow, H.H. Blau, J. Am. Ceram. Soc. 34 (1951) 165.
[20] M. Micoulaut, M. Bauchy, Phys. Status Solidi B 250 (2013) 976.
[21] J. Horbach, W. Kob, Phys. Rev. B 60 (1999) 3169.
[22] L. Xu, F. Mallamace, Z. Yan, F.W. Starr, S.V. Buldyrev, H.E. Stanley, Nat. Phys. 5 (2009) 565.
[23] J.C. Mauro, A.J. Ellison, J. Non-Cryst. Solids 357 (2011) 3924.
[24] S.R. Becker, P.H. Poole, F.W. Starr, Phys. Rev. Lett. 97 (2006) 055901.
[25] J.C. Phillips, J. Non-Cryst. Solids 182 (1995) 155.
[26] J.C. Phillips, Rep. Prog. Phys. 59 (1996) 1133.
[27] R. Friedberg, J.M. Luttinger, Phys. Rev. B 12 (1975) 4460.
[28] P. Grassberger, I. Procaccia, J. Chem. Phys. 77 (1982) 6281.
[29] R. Welch, J. Smith, M. Potuzak, X. Guo, B. Bowden, T. Kiczenski, D. Alla, S. King, A. Ellison, J.C. Mauro, Phys. Rev. Lett. 110 (2013) 265901.
[30] Y. Yu, M. Wang, D. Zhang, B. Wang, G. Sant, M. Bauchy, Phys. Rev. Lett. 115 (2015) 165901.
[31] J.C. Mauro, E.D. Zanotto, Int. J. Appl. Glas. Sci. 5 (2014) 2.